Effect of Nd(422) Dopant on the Superconducting Properties of Nd(123) Superconductor Melt-Processed in Air

Ahmed Salem Mahmoud

***Abstract*—The effect of $Nd_{3.6}Ba_{2.4}Cu_{1.8}O_{5-\delta}$ [Nd(422)] dopant on the microstructure and superconducting properties of $Nd_{0.9}Ba_{2.1}Cu_3O_{7-\delta}$ [Nd(123)] superconductor melt-processed in air has been studied using various techniques. It has been confirmed that the addition of Nd(422) phase prior to melt-processing significantly enhances the superconducting prosperities of Nd(123) superconductor when melt-processed in air atmosphere. Microstructure analysis using an electron probe micro-analyzer revealed the presence of Nd(422) inclusions in the 123 matrix and these inclusions are better dispersed and more refined in the doped sample. Compared to the undoped sample, the Nd(422)-doped sample showed significant improvement of current density at low fields with largely depressed fishtail peak effect at high temperatures. These results are ascribed to the effect of Nd(422) phase, which yet unoptimized to serve as efficient pinning centers and also allow the introduction of sufficient field induced pinning centers in the sample.**

***Index Terms*—Superconducting materials, flux pinning, critical current, high temperature superconductors.**

I. Introduction

MELT-PROCESSED Nd-Ba-Cu-O [Nd(123)] superconductors exhibit high critical temperature (T_c) and large current density (J_s) under applied magnetic fields, thus they are attractive candidates for bulk superconducting applications [1]. When these materials are melt-processed in air, however, Nd^{+3} could substitute on the Ba^{+2} sites which severely deteriorate the superconducting properties [1]. Several approaches have been developed to overcome this problem [2]–[4]. One successful approach has been the application of the so-called oxygen controlled melt growth (O-C-M-G) process [2] which is the melt-processing under controlled oxygen partial pressure. Another approach is the post heat-treatment of the melt-grown material at high temperature in flowing oxygen and argon [3]. Both approaches, however, involve complications rendering them cost ineffective. In a promising approach, Kojo *et al* reported that the addition of Ba-rich Nd(422) phase prior to the melt-processing of Nd(123) does successfully suppress the substitution effect, with high-T_c Nd(123) superconductors having been reported [4]. Similar results have been reported even with different Ba-rich compositions such as Nd(242) [5]–[8]. On the other hand, the substitution of Nd on Ba sites is desirable when it occurs on an optimum level because it could give rise to compositional fluctuations in the matrix which are known to serve as field-induced pinning centers at relatively large fields [1]. In this work, I report upon detailed investigation for the effect of Ba-rich Nd(422) dopant on the microstructure, superconducting and pinning properties in the air-melt-processed Nd(123) superconductors.

Manuscript received September 18, 2017; accepted January 12, 2018. Date of publication January 24, 2018; date of current version February 13, 2018. This work was supported by the Libyan Ministry of Higher Education.

The author is with the Department of Physics, Faculty of Science, University of Tripoli, Tripoli, Libya (e-mail: as-mahmoud@hotmail.com).

Color versions of one or more of the figures in this paper are available online at http://ieeexplore.ieee.org.

Digital Object Identifier 10.1109/TASC.2018.2797298

II. Experimental

Nominal compositions of $Nd_{0.9}Ba_{2.1}Cu_3O_{7-\delta}$ [Nd(123)] and $Nd_{3.6}Ba_{2.4}Cu_{1.8}O_{5-\delta}$ [Nd(422)] were independently prepared using the conventional-solid state reaction method. These compositions were then used to produce two Nd(123) and [Nd(123) + 10wt.%Nd(422)] precursors called Nd0 and Nd4 respectively. Each precursor was hand-pressed in a rectangular-alumina frame and sintered at 980 °C in air atmosphere to fabricate a bar. This bar was then cut into halves and melt-processed in a vertical furnace in air as described in [9]. Small samples with exposed *a-b* planes were cleaved from each melt-processed block using surgical blade and light tapping and annealed in 1-atmosphere of oxygen for 880 h between 475 °C and 250 °C. Microstructure characterization was performed using an electron probe micro-analyzer (EPMA), while the *ac* magnetic susceptibility was measured using home-made susceptometer. The magnetic hysteresis loops were measured over the temperature range 60 K $\leq$ T $\leq$ 77 K using a commercial superconducting quantum interference design (SQUID) equipped with $\pm$7 T magnet. In all cases, the magnetic field (B) was applied field parallel to the *c*-axis of the sample, B // c. The current density was measured using the Bean method [10].

III. Results and Discussion

Fig. 1 shows an optical photograph of a typical melt-textured bar fabricated in this study. The bar contained large blocks of an average length >15 mm. Single block bars with a length >35 mm have also been fabricated as typically shown in the same figure. Each block comprises stacks of grains oriented along their *c*-axis. As these blocks were fabricated in air without any seeds or contacts, they are free of contamination and their production cost is significantly reduced as compared to

Fig. 1. Optical photographs of Nd(123) melt-processed bars containing single block (top) and multiple blocks (bottom). Arrows indicate blocks.

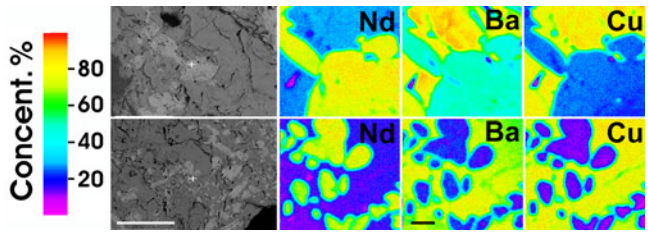

Fig. 2. Digitally enhanced, back-scattered electron micrographs (black and white) and EPMA compositional mapping images (colored) acquired from the *ab*-plane of the Nd0 (top row) and Nd4 (bottom row) samples. White and black bars correspond to 100 μm and 10 μm lengths, respectively.

their counterparts fabricated using other melt-processing techniques. It is important to indicate that the bulk application of high temperature superconductor require these materials to have large size, perfect texturing, and high and uniform bulk current density with low cost [11]. Thus, the current blocks should be quite interesting from both fundamental research and application perspectives, and if these materials could carry sufficiently large currents, they should be attractive for certain bulk applications especially the high field ones.

Fig. 2 shows back-scattered electron micrograph together with compositional mapping images obtained from carefully selected regions (50 μm $\times$ 50 μm) in the surfaces of Nd0 and Nd4 samples. In this figure, it is clear that there are two different phases corresponding to the Nd(422) inclusions (white color) and the Nd(123) matrix (dark color). The ND(422) inclusions are better refined and dispersed in the doped sample (Nd4) than they are in the undoped sample (Nd0). Thus, the addition of Ba-rich Nd(422) could improve the morphology of the Nd(422) inclusions.

Fig. 3 displays plots for the temperature dependence of *ac* susceptibility for Nd0 and Nd4 samples [6]. As can be seen from the figure, the doping process has remarkably improved the superconducting properties and largely suppressed the formation of the low-T_c phase in the sample. For the undoped sample, the transition into the superconducting state was markedly broad with two-steps. For the doped sample, the onset T_c value is ~95 K with a transition width of <2 K. These

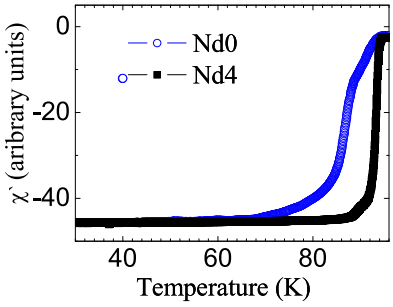

Fig. 3. Temperature dependent *ac* susceptibility curves for the Nd0 and Nd4 samples.

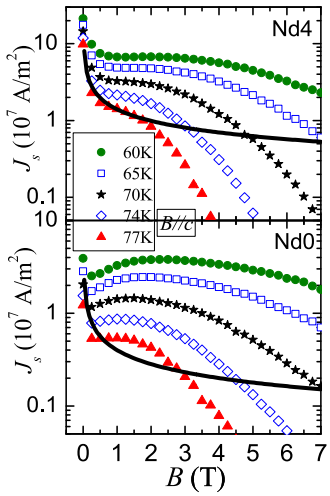

Fig. 4. Plots for the field dependence of current density (J_s) at different temperatures for Nd0 and Nd4 samples. Solid lines are fits to the data.

values are comparable to those obtained for OCMG- Nd(123) superconductors [1].

Fig. 4 shows semi-log plots of the magnetic field dependence of current density (J_s) over the temperature range 60 K $\leq$ T $\leq$ 77 K for both Nd0 and Nd4 samples The data were extracted from magnetic hysteresis loops measured using SQUID magnetometer with B // c. Clearly, the doped sample exhibits larger current density over all temperatures particularly at low fields, with smaller irreversibility fields and largely suppressed fishtail peak effect as compared with the undoped sample. However, in the undoped sample the fishtail peak is well-developed even at high temperatures. The enhanced current density at low fields and high temperature may be ascribed to the improved morphology of the Nd(422) inclusions. To strengthen this argument, I fitted the high temperature data with the power-law form $J_s(B) \sim B^{-0.5}$ known to describe surface pinning provided by normal-conducting particles [12]. The results are typically shown in Fig. 4 for T = 77 K. It is clear from this figure that, the data can be fitted very well with the form for the doped sample, while the fitting is really poor for the undoped one. The development of fishtail peak requires essentially sufficient field-induced pinning centers in the sample. The shape of the peak, is dependent on the size of the Nd(422) inclusions [13]. For high-T_c superconductors, the main defect structures responsible for the peak are Oxygen vacancies and/or compositional

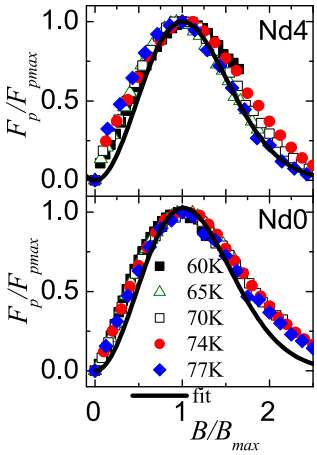

Fig. 5. Scaling of normalized pinning force $(F_p/F_{p,\max})$ versus normalized applied field $(B/B_{\max})$ for Nd0 and Nd4 samples with $B \,//\, c$.

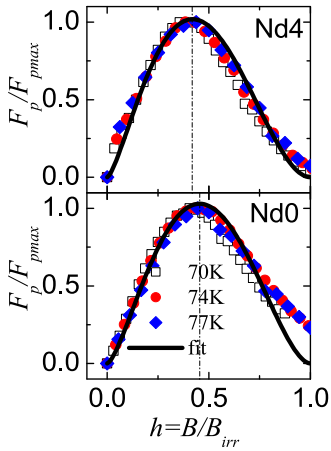

Fig. 6. Scaling of normalized pinning force $(F_p/F_{p,\max})$ versus reduced applied field $(B/B_{\rm irr})$ for Nd0 and Nd4 samples with $B \,//\, c$.

fluctuations arising from exchange effects (e.g., Nd/Ba) [13]. As the current samples were exposed to prolonged oxygen program, thus the peak cannot be explained by an oxygen effect solely. Rather, the peak seems to arise mainly from compositional fluctuations in the matrix due to Nd/Ba substitution [13]. These point-like defects, besides the oxygen vacancies, could serve as field-induced pinning centers leading to the formation of the fishtail peak. Thus, the absence/presence of the peak may be understood in terms of the scale of Nd/Ba substitution which seem to be quite small in the doped sample.

Fig. 5 shows scaling of the pinning force density normalized by the maximum pinning force density, $f = (F_p/F_{p,\max})$, versus the magnetic field normalized by the maximum field, $b_f = (B/B_{\max})$, over the temperature range 60 K $\leq$ T $\leq$ 77 K, for the Nd0 and Nd4 samples. The data were calculated from Fig. 4, with $B \,//\, c$. This scaling is equivalent to the scaling of $(J_s/J_{\max})$ versus $(B/B_{j\max})$, where $J_{\max}$ and $B_{j\max}$ are the maximum current density and its corresponding field respectively [14]. It is clear from this figure that the data is well scaled particularly around the fishtail peak region implying that the peak is formed due to a single pinning mechanism. By setting $m = 1$ and using n as a free parameter, best fits of data using the functional form (1):

$$f(b_f) = b_f^{m+1} \exp\left[\frac{m+1}{n}\left(1 - b_f^n\right)\right] \tag{1}$$

yield $n = 1.3$ and $n = 2$ for the Nd0 and Nd4 samples respectively. These values fall within the range $1 \leq n \leq 2$ found to fit a large number of different RE(123) systems [14].

Fig. 6 presents the scaling of pinning force density normalized by the maximum pinning force density $f = (F_p/F_{p,\max})$ versus the field normalized by the irreversibility field $(h = B/B_{\rm irr})$ over the temperature range 60 K $\leq$ T $\leq$ 77 K for both Nd0 and Nd4 samples, with $B \,//\, c$. It is clear from this figure that, almost all data collapse onto a universal curve thus a single pinning mechanism is dominant in these samples. Best fits of data using the well-known functional dependence (2):

$$f(h) = F_p/F_{p,\max} = Ah^p(1-h)^q \tag{2}$$

yield: $A = 10.8$, $p = 1.5$, $q = 1.99$ for the undoped sample and $A = 9.5$, $p = 1.4$, $q = 1.99$ for the doped sample (Nd4) sample. Thus the position of the maximum scaled force, (h_0), is $h_0 = p/(p+q) \sim 0.42 - 0.44$ for both samples. Based on Dew-Hughes model [15], the position of h_0 with 0.40 on the reduced field coordinate is a clear indication that the dominant pinning mechanism is of δT_c-pinning type and this mechanism is provided by superconducting defects causing spatial fluctuation of T_c [13]. It is reasonable to ascribe these defects to compositional fluctuations in the matrix due to the substitution of Nd on Ba sites.

It is worth mentioning that even though similar results have reasonably been obtained for other samples cleaved from the same block, further investigations are still needed to determine whether or not these results can represent most of the grains in the bar.

IV. Conclusion

The effect of Ba-rich Nd(422) dopant on the microstructure and superconducting properties of in-air melt-processed Nd(123)] superconductor has been investigated using various techniques. It has been found that, the addition of Ba-rich Nd(422) phase prior to the melt-processing of Nd(123) material, significantly enhances the superconducting and pinning properties of the Nd(123) superconductor. Furthermore, the Nd(422) dopant appeared to improve the morphology of the Nd(422) inclusions with enhanced current density at low fields. Scaling of the normalized pinning force density versus normalized applied magnetic field showed that the dominant pinning mechanism is provided by a scatter of T_c (δT_c-pinning type) caused by superconducting defects. These defects are ascribed mainly to compositional fluctuations in the matrix due to Nd/Ba substitution.

Acknowledgment

The author would like to thank M. Murakami and M. R. Koblischka from SRL-ISTEC, Tokyo, Japan, for their hospitality and technical assistance during SQUID measurements. The susceptibility measurement and EPMA analysis were performed at the School of Physics, UNSW, Sydney, Australia.

REFERENCES

[1] M. Murakami, N. Sakai, T. Higuchi, and S. I. Yoo, "Melt-processed light rare earth element - Ba–Cu–O," *Supercond. Sci. Technol.*, vol. 9, no. 12, pp. 1015–1032, Dec. 1996.

[2] S. I. Yoo, N. Sakai, H. Takaichi, T. Higuchi, and M. Murakami, "Melt processing for obtaining $NdBa_2Cu_3O_y$ superconductors with high T_c and large J_c," *Appl. Phys. Lett.*, vol. 65, no. 5, pp. 633–635, Aug. 1994.

[3] A. M. Hu, S. Jia, H. Chen, and Z. Zhao, "Superconducting behaviours of melt textured $Nd_{1+x}Ba_{2-x}Cu_3O_y$ undergoing heat treatments in flowing argon and oxygen," *Physica C*, vol. 272, nos. 3–4, pp. 297–300, Dec. 1996

[4] H. Kojo, S. I. Yoo, and M. Murakami, "Melt processing of high-T Nd–Ba–Cu–O superconductors in air," *Physica C*, vol. 289, nos. 1–2, pp. 85–88, Aug. 1997.

[5] A. S. Mahmoud and G. J. Russell, "Melt-processing of Nd(123)-based composites in air," presented at the 23th Australia New Zealand Condens. Matter Phys. Meeting, Wagga Wagga, Australia, Feb. 1999.

[6] A. S. Mahmoud and I. S. Ibrahim, "Microstucture and superconducting properties of $NdBa_2Cu_3O_{7-\delta}$ melt-processed in air," in *Proc. 4th Arab Conf. Mater. Sci.*, Tripoli, Libya, 2005, pp. 294–297.

[7] B. Peng, L. Cheng, Y. Zhuang, H. Xu, and X. Yao, "Large size and high Tc, Jc SmBCO bulk superconductor with addition of Sm242 particles grown in air," *Physica C*, vol. 496, pp. 11–13, Jan. 2014.

[8] B. Li *et al.*, "Materials process and applications of single grain (RE)-Ba-Cu-O bulk high-temperatuer superconductors," *Physica C*, vol. 482, pp. 50–57, Nov. 2012.

[9] A. S. Mahmoud and G. J. Russell, "Large crystals of the composite Y/Nd(123) containing various dopants grown by melt-processing in air," *Supercond. Sci. Technol.*, vol. 11, no. 10, pp. 1036–1040, Oct. 1998.

[10] C. P. Bean, "Magnetization of hard superconductors," *Phys. Rev. Lett.*, vol. 8, nos. 6–15, pp. 250–252, Mar. 1962.

[11] IFM Consultancy and Education Services, "Report of the roadmapping workshop: Bulk superconductivity," Univ. Cambridge, Cambridge, U.K., Jun. 2016, pp. 2–39. [Online]. Available: https://www.repository.cam.ac.uk/handle/1810/256650

[12] T. Matsushita, "Effect of short coherence length along the c -axis on the irreversibilty line in high-T_c superconductors," *Physica C*, vol. 205, nos. 3–4, pp. 289–295, Feb. 1993.

[13] A. S. Mahmoud, G. J. Russell, M. R. Koblischka, N. Chikumoto, and M. Murakami, "Characterization of pinning in (Y, Nd)$Ba_2Cu_3O_{7-\delta}$ melt-textured superconductors," *Physica C*, vol. 415, nos. 1–2, pp. 40–50, Nov. 2004.

[14] M. Jirsa and L. Pust, "A comparative study of irreversible magnetisation and pinning force density in RE Ba Cu O and some other high-T_c compounds in view of a novel scaling scheme," *Physica C*, vol. 221, nos. 1–2, pp. 17–24, Nov. 1997.

[15] D. Dew-Hughes, "Flux pinning in mechanisms in type II superconductors," *Philos. Mag.*, vol. 30, no. 2, pp. 293–305, Mar. 1974.